Progress In Electromagnetics Research M, Vol. 104, 61–70, 2021

Design and Implementation of an Integrated Switched-Oscillator Impulse Generator

Samira Mohammadzamani and Behzad Kordi*

Abstract—An integrated wireless impulse generator has been designed, simulated, fabricated, and tested. Switched oscillator topology has been used as an impulse generator. A switched oscillator consists of a low impedance transmission line, which is charged by a DC source with a large input impedance. The transmission line is connected to a fast closing switch at one end and a high feed-point impedance antenna at the other end. After charging the transmission line, closing the fast switch short circuits the transmission line, resulting in a transient wave propagating toward the antenna. The mismatch between transmission line characteristic impedance and the antenna feed point impedance causes a reflection at the antenna terminal. Due to the short circuit at switch terminal, the reflected signal will reflect back at the switch terminal as well. This back and forth reflection generates a series of pulses at the antenna terminal which will be radiated by the antenna. The switched oscillator impulse generator is designed to operate in the industrial, scientific and medical (ISM) radio frequency band.

1. INTRODUCTION

Wireless passive sensors have been developed recently in the industrial application for the measurement of parameters such as temperature, pH, or pressure [1–4] and will play an important role in the development of future technologies [5]. Most wireless, passive sensors rely on detecting the variation of the resonance frequency of a resonator due to a change in the measurand (e.g., [6]). These sensors are passive, which means that they do not require any power source, and they can be interrogated remotely. These low cost, passive, low weight, and wireless sensors propose new advantages compared to conventional measurement methods.

The passive, wireless, cavity-based sensors require a remote interrogation system to excite them and then receive the measurement data form the sensor. A typical interrogation system sends a single-frequency radio frequency (RF) signal to the resonator and receives the ring backs from the resonator and detects the variation of the resonance frequency of the sensor. The main part of the interrogator is a single-frequency RF source that generates RF pulses and transmits the pulses to the sensor. A low cost, compact, wireless impulse generator is proposed in this research. Unlike traditional interrogation techniques, the impulse generator developed in this work transmits a transient pulse that covers the frequency range of interest. This impulse generator consists of a switched oscillator that generates a transient pulse to excite and transmit to the wireless passive sensor.

The fundamentals of switched oscillators were first introduced by C. E. Baum in 2000 [7]. A switched oscillator consists of a low impedance transmission line (with a characteristic impedance of Z_0) charged by a DC source (V_{DC}) through a impedance (Z_S) that is large enough at desired frequencies (to block any effect of the DC source on the signal) and terminated by a high impedance antenna (Z_A) at one end and a fast closing switch (S) at the other end. The general schematic of a switched oscillator is presented in Figure 1. Once the line is charged, the switch S will close and short-circuit the transmission

Received 3 June 2021, Accepted 9 August 2021, Scheduled 15 August 2021
* Corresponding author: Behzad Kordi (behzad.kordi@umanitoba.ca).
The authors are with the Department of Electrical and Computer Engineering, University of Manitoba, Winnipeg, MB, Canada.

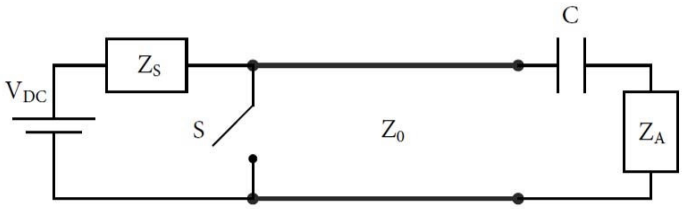

Figure 1. Schematic of a switched oscillator [7].

line. Therefore, a fast transient will be generated and travels along the transmission line. Because of the mismatch between the antenna and the transmission line, only a part of fast transient wave will be radiated and a portion of the fast transient wave will reflect back. At the other end of the transmission line, there is a closed switch. Consequently, a second reflection with reversed sign will propagate toward the antenna and the wave continues to travel back and forth. Hence, at the terminal of antenna, there will be a series of positive and negative pulses with descending amplitude [8]. The center frequency of these pulses is determined by the the length of transmission line, as each cycle of the generated pulse is equal to 4 times the delay of the transmission line [9]. Therefore, the center frequency is given by

$$f_c = \frac{v_p}{4L} \tag{1}$$

where v_p is the propagation speed of waves on the transmission line of length L.

In [10], an electromagnetic simulation in the frequency domain is employed to relate the parameters of a coaxial-transmission line-based switched oscillator to the properties of the radiated waveform. An improved, high power realization of such design is discussed in [11–13]. In this paper, the design, simulation, fabrication, and testing of a low-power integrated printed circuit board (PCB) switched oscillator is presented. The proposed switched oscillator is fabricated using a coplanar waveguide (CPW) transmission line that allows the integration of the radiating antenna. A gas discharge tube has been used in this low-power design that plays the role of the switch in the switched oscillator and mitigates the issues involved with a spark gap used in the existing designs [11–13].

The organization of the paper is as follows. The simulation model of the switched oscillator and a sensitivity analysis of the model is presented in Section 2. Section 3 details the fabrication and testing of the designed switched oscillator. Finally, the concluding remarks are presented in Section 4.

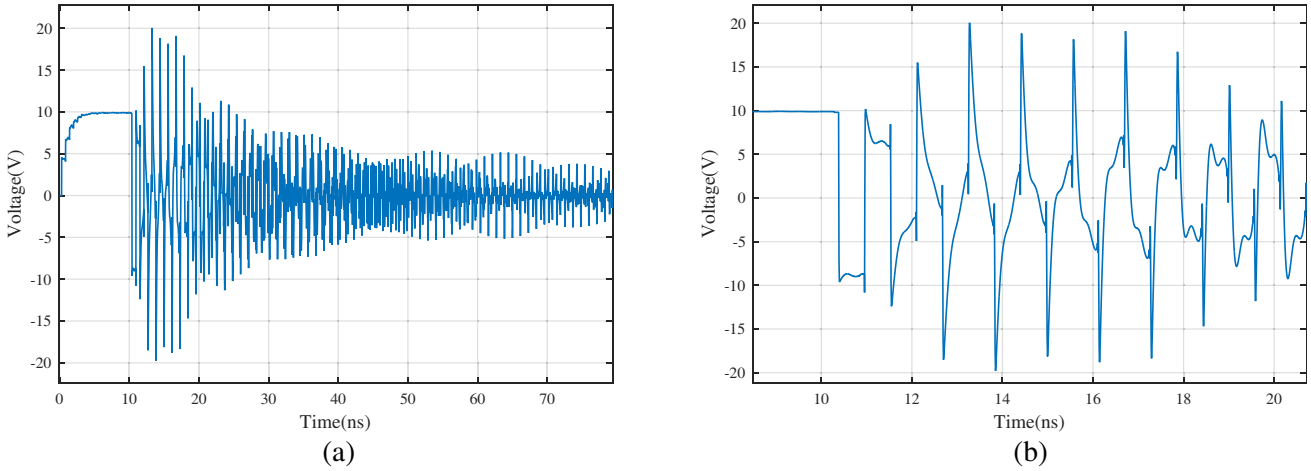

Figure 2. Time-domain simulation result of a switched oscillator with a resonance frequency of 915 MHz, (a) 0–80 ns window, (b) zoomed-in 5–20 ns window.

2. SIMULATION MODEL

The time-domain simulation was performed on the switched oscillator. The input is a 10-V DC source, the switch transition time is 100 ps, and the transmission line is 5.8 cm long with a characteristic impedance of 15 Ω. As the antenna model, an equivalent circuit model with an impedance equal to the input impedance of a dipole antenna has been used. A circuit representing the input impedance of the antenna was determined by fitting the input impedance of the antenna as a rational function and synthesizing it as a multi-branch RLC circuit.

The output voltage has been determined at the antenna feed point. The time domain simulation result is represented in Figure 2. This figure shows the time domain result for 70 ns and Figure 3 shows the frequency content of the voltage waveform. As the figure demonstrates the center frequency is 918.1 MHz and the 3 dB band width is 9.3 MHz.

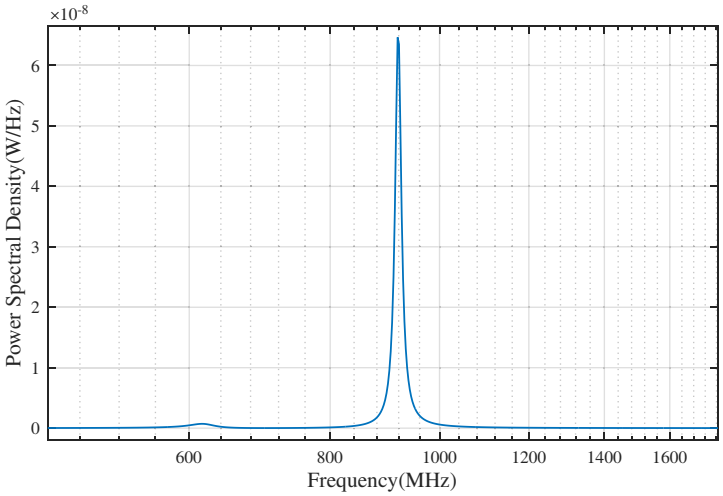

Figure 3. Frequency domain simulation result of a switched oscillator with resonance frequency of 915 MHz.

To identify the effects of any changes or tolerances in design parameters on the switched oscillator output signal, some sensitivity tests were performed.

(i) **Variation in length of the transmission line by ±10%:** Figure 4 depicts the time domain and

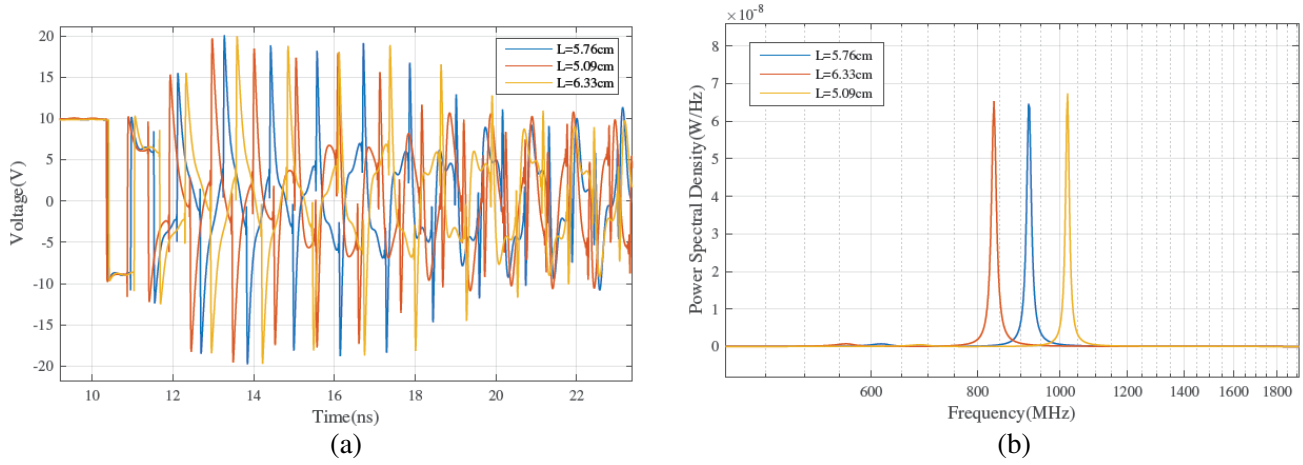

Figure 4. Simulation results of a switched oscillator with different transmission line lengths in (a) time domain and (b) frequency domain.

frequency domain result of the simulations. As expected, a change in the length of transmission line caused change in the center frequency of the switched oscillator. 10% increase in the transmission line length leads to 9.5% decrease in the center frequency and 10% decrease in the transmission line length makes the center frequency increase by 9.4%. The bandwidth and amplitude of the signal stay almost the same.

(ii) **Variation in characteristic impedance of the transmission line by ±30%:** The results of the time-domain and frequency-domain simulations using transmission lines with 10, 15, and 20-Ω characteristic impedance are shown in Figure 5. As this figure shows, by 30% reduction of the characteristic impedance of the transmission line, the amplitude of the power spectral density of the signal drops by 38% and by 30% increasing the characteristic impedance of the transmission line, the amplitude of the power spectral density of the signal rises by 105% which matches our expectation from theory that smaller characteristic impedance of the transmission line leads to higher reflection coefficient at antenna terminal and consequently higher amplitude of the signal.

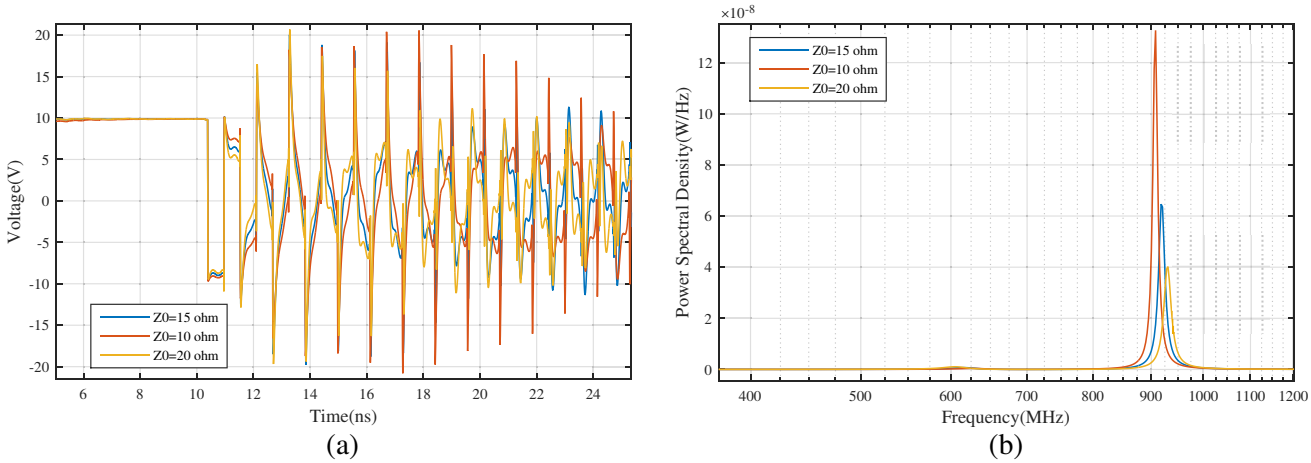

Figure 5. Simulation results of a switched oscillator with different transmission line characteristic impedance in (a) time domain and (b) frequency domain.

(iii) **Variation in length of the antenna by ±10%:** The length of the antennas is varied by ±10%. Therefore, the resonance frequency of the antenna changes. Figure 6 is illustrating the time domain

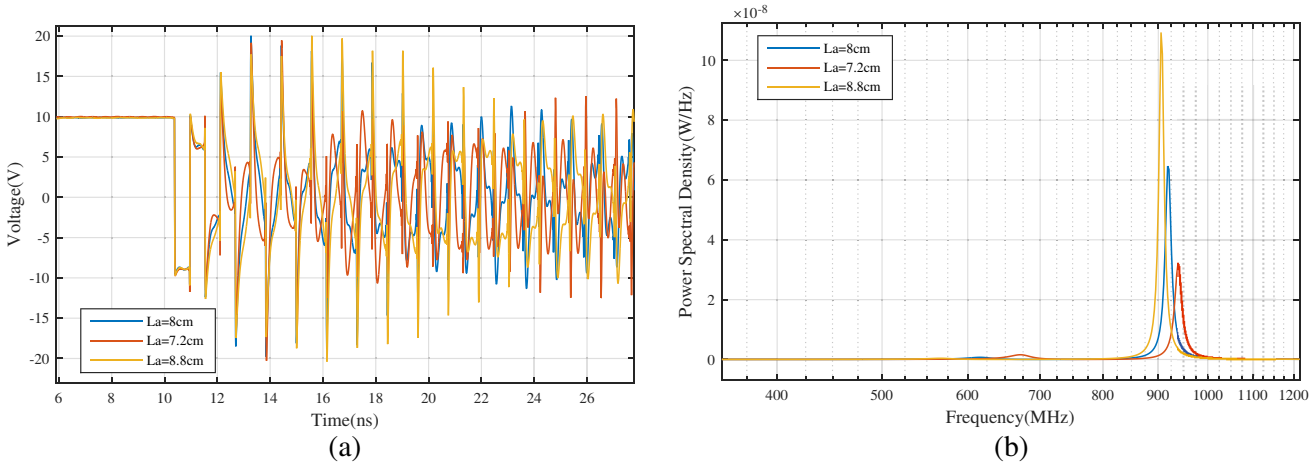

Figure 6. Simulation results of a switched oscillator with different lengths of the antenna in (a) time domain and (b) frequency domain.

and frequency domain results of the three simulations. As the this figure shows, variation of the length of the antenna causes a slight change in the center frequency of the signal generated by the switched oscillator. Increasing the length of the antenna by +10% leads to +2.8% raise in the center frequency of the signal generated by the switched oscillator and reducing the length of the antenna by −10% leads to −1% decrease in the center frequency of the signal generated by the switched oscillator.

(iv) **Increasing switch transition time to** 1 **and** 2 **ns:** Switch transition time of 0.1, 1, and 2 ns was studied. Figure 7 presents the time domain and frequency domain results of the three simulation cases. As the figure shows, up to a 1 ns transition time the impact of the variation of the switch transition time on the signal is negligible; however, the transition time more than 1 ns causes fluctuation in the center frequency of the signal.

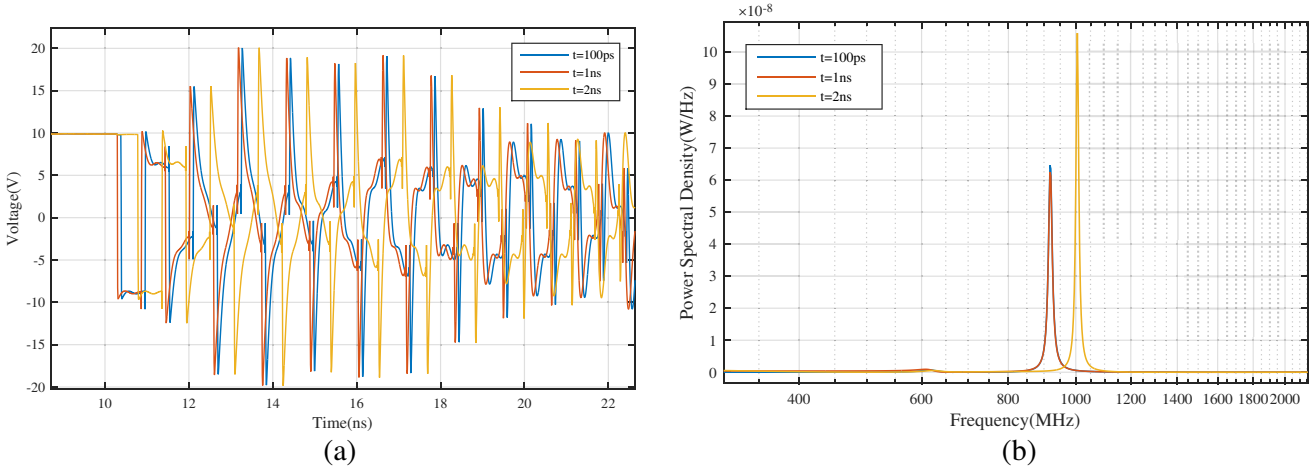

Figure 7. Simulation results of a switched oscillator with different switch transition times in (a) time domain and (b) frequency domain.

(v) **Effect of antenna feed point impedance:** A dipole antenna and a monopole antenna were chosen for the simulations where the feed point impedance of the dipole antenna is twice the feed point impedance of the monopole antenna. Figure 8 demonstrates the time domain and the frequency domain of the simulations results. The results show that the dipole antenna leads to

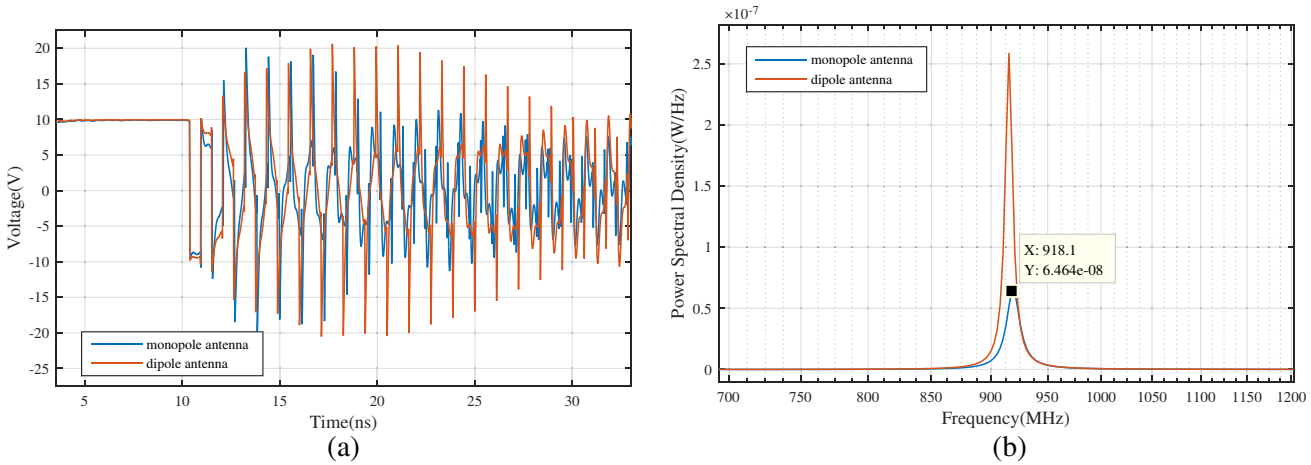

Figure 8. Simulation results of a switched oscillator with different antenna feed point impedance in (a) time domain and (b) frequency domain.

higher amplitude of the pulses and consequently higher power spectral density of the signal than the monopole antenna. This is because of the higher feed point impedance of the dipole antenna which makes the reflection coefficient larger, and therefore the amplitude of the reflected signal toward the switch is higher. By increasing the feed point impedance of the antenna by +100% the amplitude of the power spectral density of the signal rises by +302%. Using dipole antenna instead of monopole antenna also induced a slight change (−0.3%) in the center frequency.

A summary of the results of the sensitivity analysis is presented in Table 1.

Table 1. Summary of the sensitivity analysis of the switched oscillator output frequency and amplitude on the design parameters.

Design variable	Nominal	Variation	Variation of the centre frequency	Variation of the amplitude
Length of transmission line	5.76 cm	+10%	−9.5%	none
		−10%	+9.4%	none
Characteristic impedance of the transmission line	15 Ω	+30%	none	−38%
		−30%	none	+105%
Length of the antenna	7.2 cm	+10%	+2.8%	none
		−10%	−1%	none
Switch transition time	1 ns	0.1 ns	none	none
		2 ns	+30%	none
Type of antenna	Monopole	Dipole	−0.3%	+302%

3. EXPERIMENTAL TEST RESULTS

3.1. Fabrication of Switched Oscillators

Two switched oscillators were fabricated in this work. The first switched oscillator consists of a coaxial-cable transmission line, a monopole antenna, a gas discharge tube (Littelfuse 2027 series) as the switch, an RF choke, and the DC charging circuit. In the second switched oscillator, a conductor backed coplanar waveguide (CBCPW) connected to a printed monopole antenna was fabricated. To fabricate the CBCPW with a 15-Ω characteristic impedance at 915 MHz the substrate RT/duroid 5870 laminate by Rogers Corporation with a dielectric constant of 2.33 and 0.787 mm thickness has been used. The

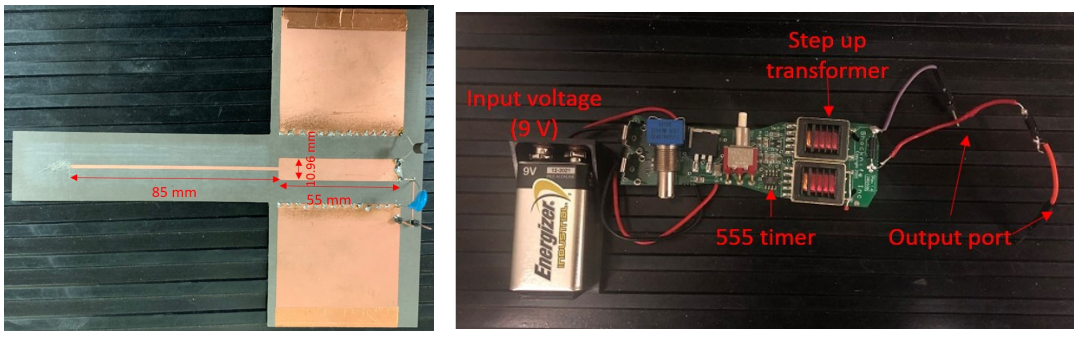

(a) (b)

Figure 9. (a) Front side of the fabricated CBCPW transmission line consisting of a 55-mm long and 10.96-mm wide strip connected to a printed monopole antenna, (b) the fly-back boost converter circuit that generates a DC voltage of about 7.5 kV.

width of the conductor strip is 10.96 mm and the gap between the conductor strip and top layer ground planes is 10 mm which is bigger than twice of the dielectric thickness (0.787 mm). The length of the transmission line is 55 mm, and the width of each top layer ground plane is 59.5 mm. The width of the bottom layer ground is 150 mm. Figure 9(a) shows the fabricated CBCPW transmission line, and the fly-back boost converter circuit that generates the kV-range DC voltage is shown in Figure 9(b).

3.2. Measuring System

The signal generated by the first switched oscillator has been measured by a commercial D-dot electric field probe (Prodyn AD-S30). The D-dot probe is a high frequency electric field sensor that measures the rate of change of the electric displacement over time in a wide range of frequency. The bandwidth of AD-S30 is more than 1 GHz, can measure a risetime of less than 0.35 ns, and its output range is up to ±4 kV. The distance between the monopole antenna and the sensor was 30 cm. Both monopole antenna and the D-dot sensor were at the same height from the ground.

A 3×3 cm parallel plate capacitive sensor with a 2 mm air dielectric has been used to measure electric field radiated by the planar switched oscillators. The parallel plate capacitive sensor was placed 10 cm above the printed monopole antenna. A schematic of the measuring system is shown in Figure 10.

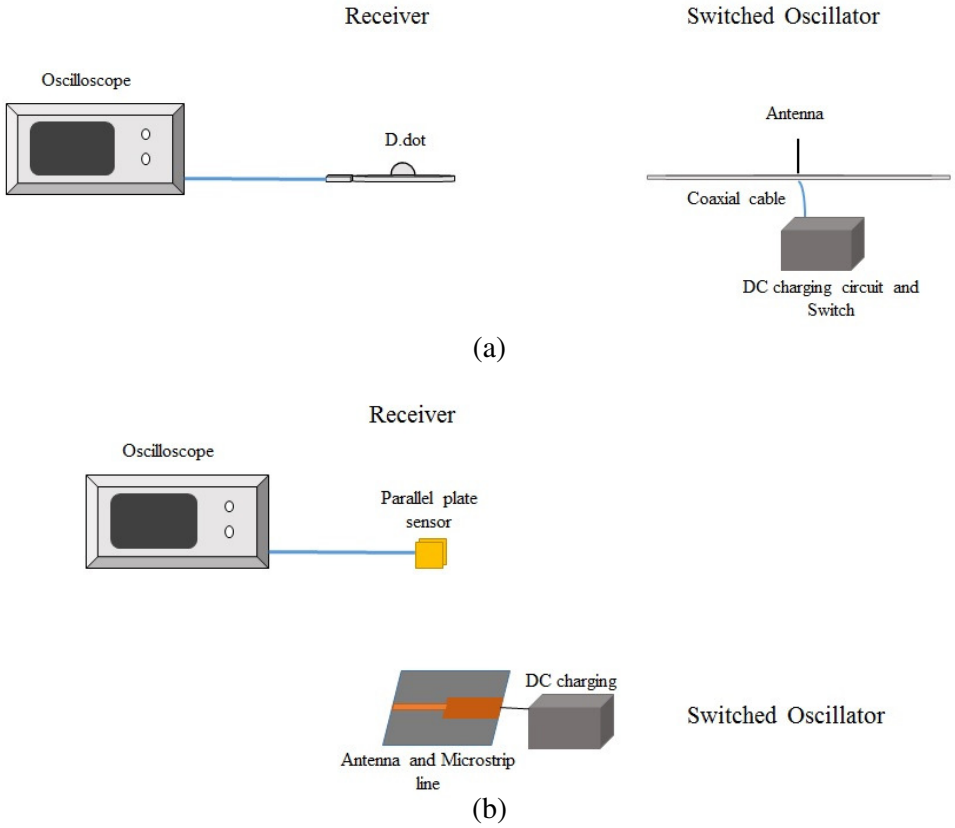

Figure 10. Experimental setup to measure the radiated electric field by the switched oscillator using (a) monopole antenna and D-dot, and (b) CBCPW transmission line and printed monopole antenna.

3.3. Measurement Results

Figure 11(a) presents the electric field of the coaxial cable switched oscillator measured with the D-dot sensor. The measured peak amplitude of the signal is 0.17 V/m. Most of the energy of the signal contains in the time interval of 3 ns to 13 ns that is because of the small mismatch between coaxial cable transmission line characteristic impedance and monopole antenna input impedance. Figure 11(b)

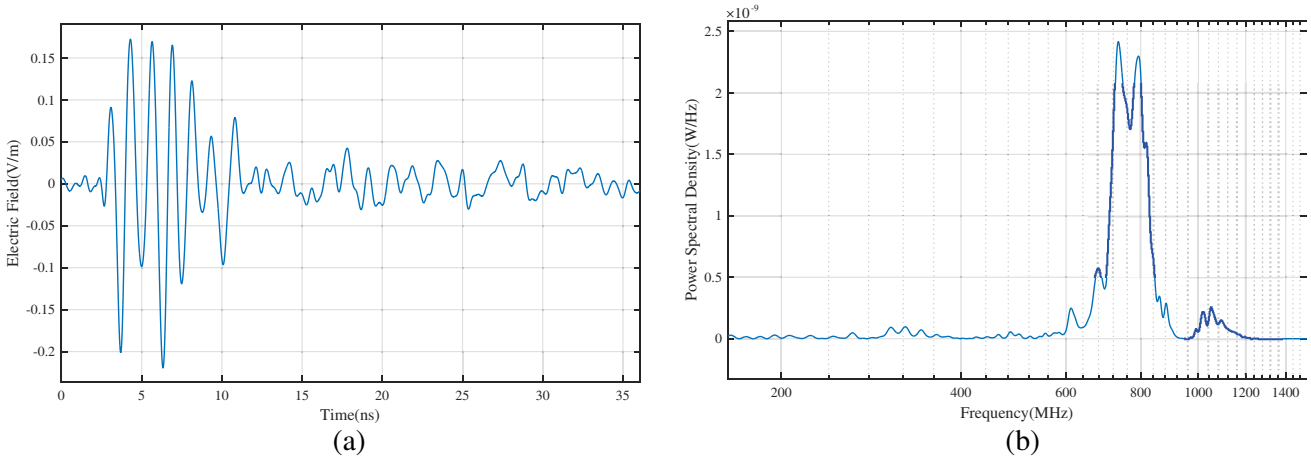

Figure 11. (a) Measurement result of the switched oscillator with coaxial cable transmission line and monopole antenna, (b) power spectrum of the measurement result.

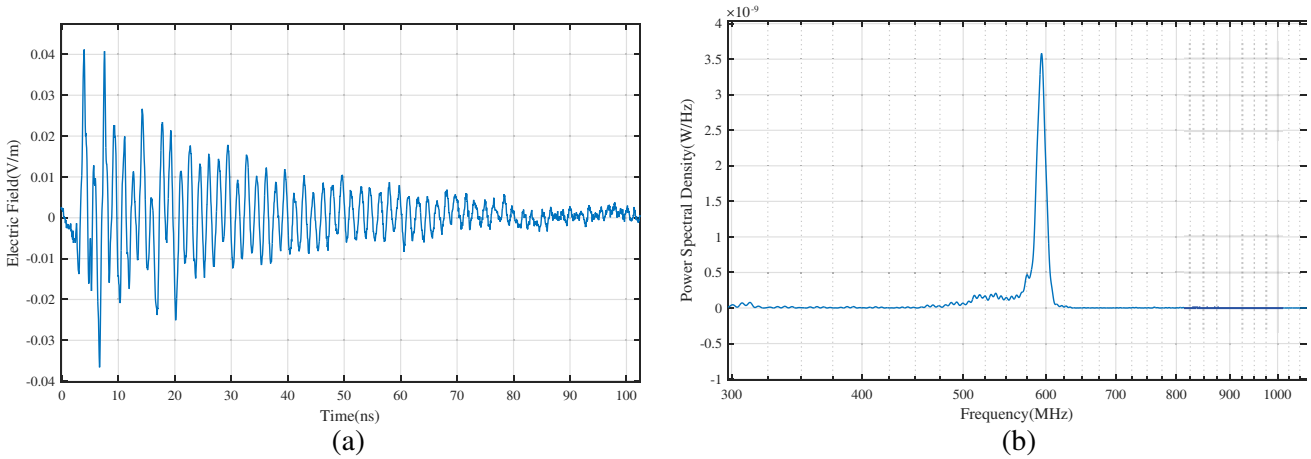

Figure 12. (a) Measurement result of the switched oscillator with CBCPW transmission line and printed monopole antenna, (b) power spectrum of the measurement result.

represents the power spectral density of the measurement results of the coaxial cable switched oscillator. As the figure depicts, the power spectral density has two peaks, very close to each other. The first peak, happens at 715 MHz and the second peak appears at 798 MHz. Both peaks are higher than the expected frequency which was 679 MHz. The reason might be the difference between the resonance frequency of the quarter wavelength coaxial cable transmission line and the resonance frequency of the monopole antenna. Adjusting the length of the monopole antenna and subsequently the first resonance frequency of the antenna results in changes in the peak frequencies.

Figure 12(a) shows the electric field measurement result of the CBCPW switched oscillator, measured by the parallel plate capacitive sensor. The measured peak amplitude of the signal is 0.04 V/m which is a lot less than the peak amplitude signal of the coaxial cable switched oscillator. The higher loss of a CBCPW transmission line than a coaxial cable transmission line is an explanation for the lower peak amplitude of the CBCPW switched oscillator signal. On the other hand, sensitivity of the parallel plate capacitive sensor is less than the D-dot electric field sensor and it could be another reason for the lower peak amplitude. The duration of the signal is about 80 ns which is more than the duration of coaxial cable switched oscillator and it is due to higher mismatch between CBCPW transmission line characteristic impedance (15 Ω) and printed monopole antenna input impedance (34 Ω). The power spectral density of the measurement results of the CBCPW switched oscillator is demonstrated in

Figure 12(b). Due to the perfect match between the resonance frequency of the quarter wavelength CBCPW transmission line and the first resonance frequency of the printed monopole antenna, power spectral density has only one peak. The resonance frequency of the CBCPW switched oscillator is 598 MHz which is not what we expect (915 MHz). The reason could be the wires that connect the DC charging circuit to the transmission line. The length of the wires adds to the length of the transmission line, resulting in decreasing the resonance frequency. In this prototype, the wires are in the shortest length possible, but they are still about 1 cm long and shift the resonance frequency to 598 MHz.

4. CONCLUSION

The design, simulation, fabrication, and assessment of a wireless integrated impulse generator are presented in this paper. A switched oscillator has been fabricated as the impulse generator. The switched oscillator is composed of a transmission line with low characteristic impedance terminated by an antenna with a higher feed point impedance at one end and a short-circuit switch at the other end.

A circuit model was developed to simulate the behavior of the switched oscillator. In the circuit model, the input impedance of the antenna was synthesized by fitting the input impedance as a rational function and realized as a multi-branch RLC circuit. The sensitivity of the switched oscillator output to the design parameters was investigated using the simulation model. Measurement results captured using the designed prototype switched oscillator have proven the applicability of the switched oscillator as a compact, wireless, pulse generator.

ACKNOWLEDGMENT

The authors are thankful to Mr. Alex McIlraith for his assistance. Financial support from Natural Sciences and Engineering Research Council of Canada (NSERC) is acknowledged.

REFERENCES

1. Tan, Q., T. Luo, T. Wei, J. Liu, L. Lin, and J. Xiong, "A wireless passive pressure and temperature sensor via a dual LC resonant circuit in harsh environments," *Journal of Microelectromechanical Systems*, Vol. 26, No. 2, 351–356, 2017.
2. Yao, J., S. Tjuatja, and H. Huang, "Real-time vibratory strain sensing using passive wireless antenna sensor," *IEEE Sensors Journal*, Vol. 15, No. 8, 4338–4345, 2015.
3. Viikari, V., J. Song, and H. Seppa, "Passive wireless sensor platform utilizing a mechanical resonator," *IEEE Sensors Journal*, Vol. 13, No. 4, 1180–1186, 2013.
4. Bhadra, S., D. S. Y. Tan, D. J. Thomson, M. S. Freund, and G. E. Bridges, "A wireless passive sensor for temperature compensated remote pH monitoring," *IEEE Sensors Journal*, Vol. 13, No. 6, 2428–2436, 2013.
5. Zhou, I., et al., "Internet of things 2.0: Concepts, applications, and future directions," *IEEE Access*, Vol. 9, 70961–71012, May 2021.
6. Yazdani, M., D. J. Thomson, and B. Kordi, "Passive wireless sensor for measuring AC electric field in the vicinity of high-voltage apparatus," *IEEE Trans. Industrial Electronics*, Vol. 63, No. 7, 4432–4441, 2016.
7. Baum, C. E., "Switched oscillators," *Circuit and Electromagnetic System Design Note*, 2000.
8. Baum, C. E., "Differential switched oscillators and associated antennas," *Circuit and Electromagnetic System Design Note*, 2001.
9. Vega, F., F. Rachidi, and D. V. Giri, "A new set of electrodes for coaxial quarter wave switched oscillators," *IEEE Trans. Plasma Science*, Vol. 41, No. 9, 2545–2550, Sep. 2013.
10. Armanious, M., J. S. Tyo, M. C. Skipper, M. D. Abdalla, W. D. Prather, and J. E. Lawrance, "Interaction between geometric parameters and output waveforms in high-power quarter-wave oscillators," *IEEE Trans. Plasma Science*, Vol. 38, No. 5, 1124–1131, Apr. 2010.

11. Vega, F. and F. Rachidi, "A switched oscillator geometry inspired by a curvilinear space — Part I: DC considerations," *IEEE Trans. Plasma Science*, Vol. 44, No. 10, 2240–2248, Jun. 2016.
12. Vega, F. and F. Rachidi, "A switched oscillator geometry inspired by a curvilinear space — Part II: Electrodynamic considerations," *IEEE Trans. Plasma Science*, Vol. 44, No. 10, 2249–2257, Jul. 2016.
13. Vega, F., F. Rachidi, N. Mora, N. Peña, and F. Roman, "Design, realization, and experimental test of a coaxial exponential transmission line adaptor for a half-impulse radiating antenna," *IEEE Trans. Plasma Science*, Vol. 41, No. 1, 137–181, Dec. 2012.